JOURNAL OF APPLIED ELECTROCHEMISTRY **29** (1999) 65–73

Electrochemical behaviour of indium ions in molten equimolar $CaCl_2$–NaCl mixture at 550 °C

Y. CASTRILLEJO*, M. R. BERMEJO, A. M. MARTÍNEZ, C. ABEJÓN

Dpto. de Química Analítica, Facultad de Ciencias, Universidad de Valladolid, Prado de la Magdalena s/n, 47005 Valladolid, Spain

S. SÁNCHEZ, G. S. PICARD

Laboratoire d'Electrochimie Analytique et Apliquée, Ecole Nationale Superiéure de Chimie de Paris, 11 rue Pierre et Marie Curie, 75231 Paris Cedex 05, France

Received 27 October 1997; accepted in revised form 10 March 1998

The stability of indium chloride and oxide as well as the electrochemical behaviour of indium ions have been studied in the equimolar $CaCl_2$–NaCl melt at 550 °C by X-ray diffraction (XRD) and different electrochemical techniques, using molybdenum and tungsten wires as working electrodes. Voltammetric and chronopotentiometric studies showed signals attributed to the presence of three oxidation states of indium, i.e. 0, I and III. The standard potential of the redox couples, as well as the solubility products of indium oxides have been determined, showing that In(III) ions are completely reduced to monovalent indium by the indium metal according to the reaction:

$$\mathrm{In(III)} + 2\,\mathrm{In} \leftrightarrow 3\,\mathrm{In(I)}$$

and that In_2O is a strong oxide donor according to the reaction:

$$\mathrm{In_2O\,(s)} \rightarrow 2\,\mathrm{In(I)} + \mathrm{O^{2-}}$$

These results have allowed the construction of E-pO^{2-} equilibrium diagrams summarising the properties of In–O compounds. The electrodeposition of indium was uncomplicated at Mo and W electrodes. Very good adherence of liquid indium to the electrode materials was observed, with the formation of Na–In alloys at highly reducing potentials, and there was no evidence of indium dissolution into the melt. Moreover, the voltammograms corresponding to the electrochemical In(III)/In(I) exchange were well defined. The two electrochemical steps were found to be quasi-reversible, and the values of the kinetic parameters, k^o and α, for both reactions, as well as the diffusion coefficients, $D_{\mathrm{In(III)}}$ and $D_{\mathrm{In(I)}}$ were calculated.

Keywords: *molten chlorides*, *indium chlorides*, *oxoacidity*, *calcium chlorides*, *kinetic parameters*

1. Introduction

Molten salts have proved to be suitable media for metal electrowinning, electrorefining and electroforming. In the last years a new field has been developed, the use of molten salt media for preparation of polycrystalline thin films of semiconducting materials for use in photoelectrochemical cells [1, 2]. The interest is due to the need for developing new low-cost techniques for the production of solar cells.

Various processing methods have been used for deposition of semiconducting materials, among which electrodeposition seems to be the most convenient, not only from an economic point of view, but also because it is possible to obtain large surfaces of materials. Moreover, this technology can be easily applied in industry. The use of molten media instead of aqueous solutions is attractive due to their high conductivity, large electroactivity range and high temperature, which ensure a good growth of the deposits.

The chalcopyrite semiconductor, $CuInSe_2$ '*CIS*', is a promising material for electrooptical, photovoltaic and photoelectrochemical applications [3–5] due to its high absorption coefficient ($10^5\,cm^{-1}$) and whose synthesis by electrodeposition in molten salts has not yet been studied. We have chosen molten chlorides in order to prepare the semiconducting materials because there is a wide knowledge of them from both a theoretical and experimental point of view. In particular we have performed our studies in the equimolar $CaCl_2$–NaCl mixture instead of the well known LiCl–KCl eutectic because, although both have a wide electrochemical range, the use of the former avoids the formation of solid-lithium compounds undesirable in the electrodeposition of semiconducting thin layers.

To determine the optimal conditions for the synthesis of '*CIS*', the knowledge of the electrode-

* Author to whom correspondence should be addressed.

© 1999 Kluwer Academic Publishers.

position process of the different elements that form the semiconducting material is needed. In this work we have carried out a study of the chemical and electrochemical behaviour of one of these metals, indium.

There have been some chemical and electrochemical studies of indium ions in molten salts. The LiCl–KCl eutectic [6–11], the equimolar mixture NaCl–KCl [12, 13], the $AlCl_3$–NaCl–KCl [14] and the $ZnCl_2$–2 NaCl mixtures [15] are the molten media most used for this kind of study. Some important differences have been found in the stability and the electrochemical properties of the different oxidation states of indium in these media. Due to this fact, as well as the lack of information concerning the behaviour of indium ions in the $CaCl_2$–NaCl mixtures, we have undertaken a systematic study of their electrochemistry in the equimolar mixture at 550 °C using different electrode materials. Thus we have studied both the In(III)/In(I) and the In(I)/In(0) electrochemical systems as well as the stability of the different In–O compounds in the melt.

2. Experimental details

2.1. *Preparation and purification of the melt*

The materials used in the experiments and the purification of the cell feed was also important in order to obtain consistent results; thus, the equimolar mixture ($CaCl_2$ and NaCl analytical grade) was melted in a 100 cm^3 alumina crucible placed in a quartz cell within a Renat furnace. The temperature of the furnace was controlled to ±2 °C by a West 3300 programmable device. All handling of the melt was made inside a glove box, MBraun Labstar 50.

The mixture was fused under vacuum, purified by bubbling dry hydrogen chloride for 30 min, and then kept under a dry argon atmosphere which removed the residual HCl and maintained an inert atmosphere. This procedure was used previously [16–23].

2.2. *Electrodes and apparatus*

Tungsten and molybdenum wires (1mm dia.) were used as working electrodes. A tungsten wire was used as counter electrode. The electrode active surface area was determined by the depth of immersion and the results were corrected for the height of the meniscus.

In the pK_s determinations, the pO^{2-} indicator electrode consisted of a tube of yttria-stabilized zirconia, supplied by Degussa (inner dia. 4 mm, outer dia. 6 mm), filled with molten $CaCl_2$–NaCl and containing oxide and silver ions in which a silver wire was immersed (inner reference Ag^+/Ag) [23, 24].

The reference electrode consisted of a silver wire (0.5 mm dia.) dipped into a quartz tube containing a 0.75 mol kg^{-1} solution of silver chloride in $CaCl_2$–NaCl.

The e.m.f. measurements were made with a high impedance voltmeter (Crison 2002). Cyclic voltammetry and pulse techniques were recorded with a PAR EG&G (model 273A) potentiostat–galvanostat interfaced to a computer using the appropriate software.

2.3. *Preparation of indium solutions*

The chemical stability of solutions is an important parameter which must be controlled to ensure reproducible electrochemical measurements.

The In(III) solution were always prepared by direct addition of weighed amounts of solid $InCl_3$ which was kept in a dry glove box until used, stored under argon atmosphere and used without further purification. For preparing In(I) solution we used a method used in other molten chlorides [25], that is, addition of $InCl_3$ in the presence of excess of metallic indium to allow the following equilibrium to be established.

$$InCl_3 + 2\,In \leftrightarrow 3\,InCl \qquad (1)$$

The progress of the reaction was followed by voltammetry.

3. Results and discussion

3.1. *Stable oxidation states of indium*

It is possible to determine the electrochemical window of the melt by recording the voltammograms of the mixture after purification using a tungsten or a molybdenum wire as working electrode [26]. Tungsten does not alloy with the alkali metals and the window is limited at positive potential by the oxidation of chloride ions to chlorine, and at negative potentials by the reduction of Na(I) ions to Na(0), at 1.233 and −2.433 V vs Ag^+/Ag, respectively. The ΔE value was calculated from the thermodynamic and experimental data in a way similar to that described previously [26]. The experimental electroactivity range is larger than the theoretical value, which indicates an electrochemical reaction overvoltage for the chloride–chlorine system. Molybdenum exhibits a high degree of electrochemical stability, but its practical oxidation potential is lower than that at which chlorine is evolved (0.300 V vs Ag^+/Ag), indicating that molybdenum can be anodically dissolved, a similar behaviour being observed in other molten chlorides [27].

A typical voltammogram for the electro-reduction of a solution of In(III) is shown in Fig. 1(a). The voltammograms presented the same general features at tungsten and molybdenum electrodes. The electroreduction of In(III) solutions takes place in two steps. In zone 1, the cathodic wave A associated with the anodic wave A′, whose shapes are characteristic of a soluble–soluble exchange, are related to the In(III)/In(I) exchange. Moreover, zone 2 shows a cathodic peak B and one sharp anodic stripping peak B′ characteristic of a system involving an insoluble compound; this corresponds to the In(I)/In(0) system. This was confirmed analysing the semiintegral of the

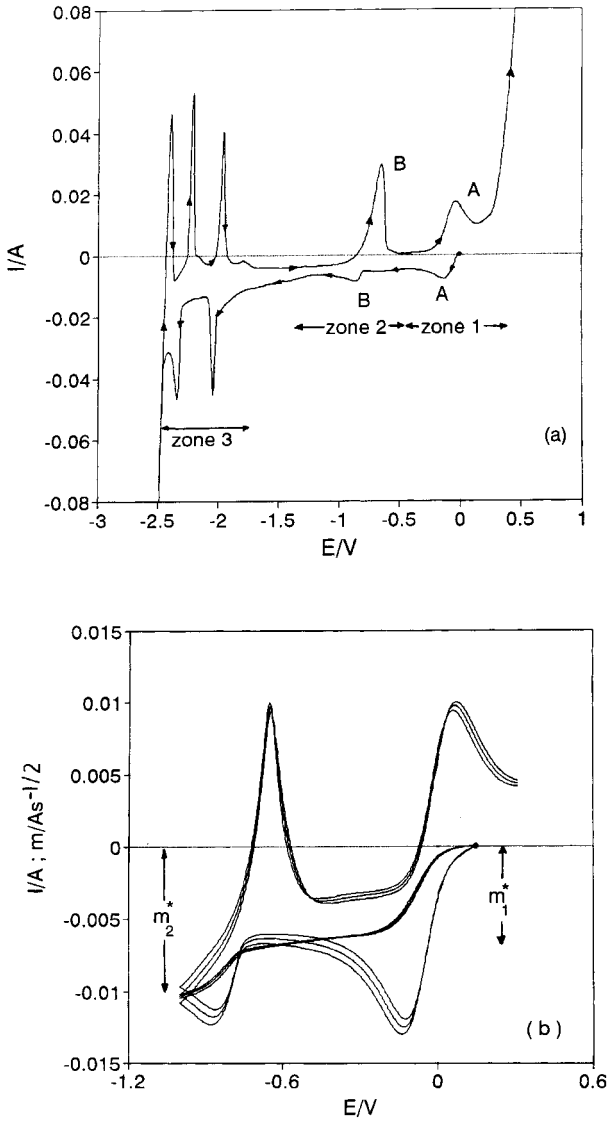

Fig. 1. (a) Typical cyclic voltammogram for the reduction of $InCl_3$, 4.201×10^{-5} mol cm^{-3} on a molybdenum electrode. Sweep rate 0.2 V s^{-1}. $S = 0.30$ cm^2. (b) Series of voltammograms related to the reduction of $InCl_3$ and their corresponding semiintegral curves. Sweep rates, v: 0.8; 0.9 and 1.0 V s^{-1}. [$InCl_3$] = 5.14×10^{-5} mol cm^{-3}. $S = 0.20$ cm^2.

voltammetric curves. When the linear potential sweep data obtained with a solution of In(III) were transformed, according to the convolution principle [28] into a form resembling a steady-state voltammetric curve, the occurrence of two plateau was evident, suggesting the existence of two electrochemical exchange steps (Fig. 1(b)). It has been shown, from theoretical considerations, [29] that

$$\frac{m_2^*}{m_1^*} = \frac{n_2 + n_1}{n_1} \qquad (2)$$

where m_1^* and m_2^* are the maximum values of the semiintegral for the first and second step, respectively, and n_1 and n_2 the corresponding electron numbers for each step. The experimental values of m_2^*/m_1^* obtained were in good agreement with an exchange of two electrons for the first reduction step, and one electron for the second.

In addition, the signals observed at highly reducing potentials, (zone 3) are attributed to the formation of Na–In alloys of different composition. The A/A′ and B/B′ exchange steps were studied separately.

3.2. *In(III)/In(I) exchange*

A detailed investigation of the In(III)/In(I) redox system (A/A′) was performed with both In(III) and In(I) solutions, using tungsten and molybdenum electrodes.

A series of cyclic voltammograms were recorded in the purified melt containing In(III) ions, for a variety of concentrations and sweep rates. Fig. 2(a) shows some voltammetric curves for the reduction of In(III) at a tungsten electrode where a linear dependence of the cathodic peak current, I_{pc}, with the square root of the sweep rate was found (Fig. 2(b)), which shows that linear semiinfinite diffusion conditions were achieved. It becomes clear that the reduction step of In(III) consist of a simple diffusion-controlled charge transfer process. From the slope of such a plot, the diffusion coefficient of In(III) was calculated by applying the Randles–Sevcik equation.

$$I_p = 0.4463\,(nF)^{3/2}(RT)^{-1/2}SCD^{1/2}v^{1/2} \qquad (3)$$

where I_p is the peak current, C the concentration of electroactive species, in this case In(III) and S is the electrode area. The values obtained are shown in Table 1.

The peak potentials do not change with increasing sweep rate for values lower than 0.3 V s^{-1} (Fig. 2(c)), a behaviour expected for a diffusion controlled process, and the slope of the plot of $\log(I_p - I)/I$ against E, over the approximate current range $0.35\,I_p - 0.7\,I_p$, approaches the theoretical value of $2.3\,nF/RT$ corresponding to a fast electrochemical process [30], whereas for higher sweep rates the slope deviates from the theoretical value and the peak potential is shifted towards negative potentials, indicating that at these conditions the electron transfer rate is significantly lower than that of mass transport.

Moreover, when analysing the convoluted voltammograms, a plateau was observed showing that mass transfer towards the electrode is diffusion controlled. The diffusion coefficient, $D_{In(III)}$, is obtained when the transformed current data reach their limiting values by applying the equation (see Table 1):

$$m^* = nFSCD^{1/2} \qquad (4)$$

The convoluted curves were very similar for increasing sweep rate, but the direct and reverse scans did not remain identical when using any of the substrates studied; this is likely due to irreversibility of the In(III)/In(I) process.

A further study of the electrochemical behaviour of indium was carried out using chronopotentiometry. The analysis of the first transition time variation

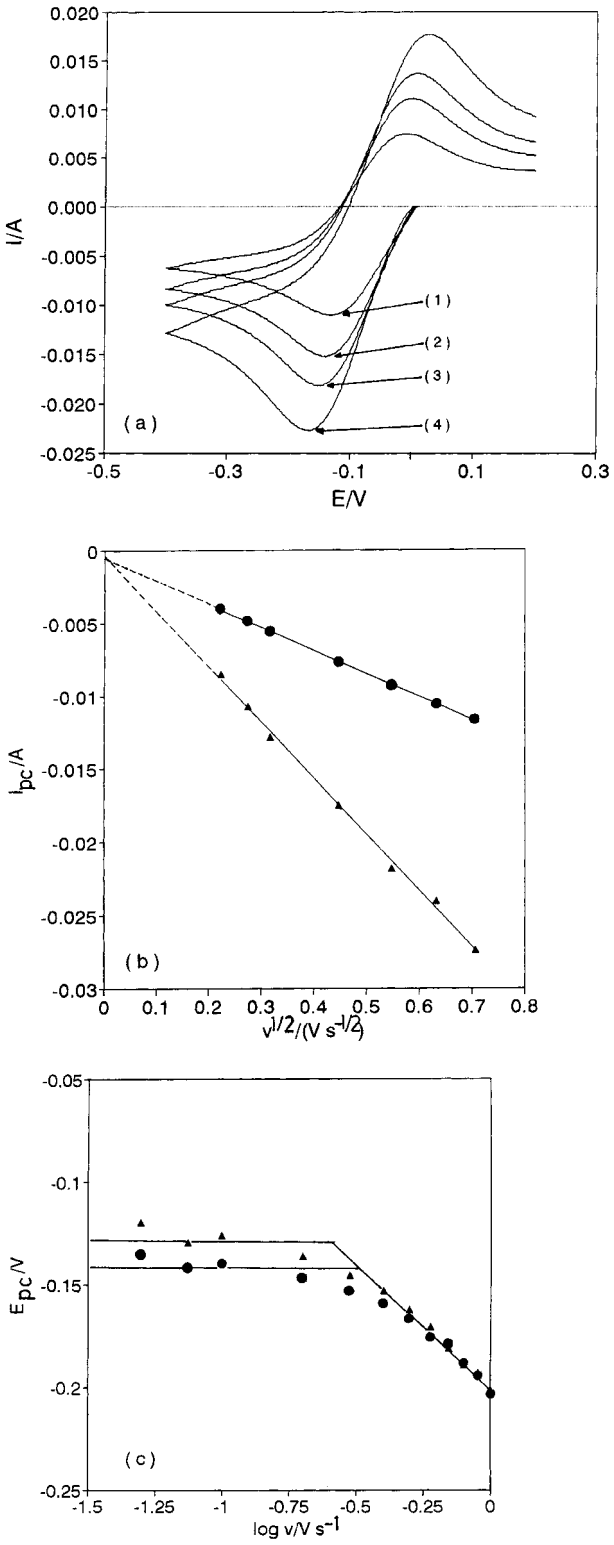

Fig. 2. (a) Cyclic voltammograms for the In(III) reduction at tungsten electrode. Sweep rates, v: (1) 0.1; (2) 0.2; (3) 0.3 and (4) 0.5 V s^{-1}. (b) Variation of the cathodic current with the square root of the sweep rate. (c) Variation of the cathodic peak potentials with the logarithm of the sweep rate. Key: (▲) tungsten and (●) molybdenum electrodes. $[InCl_3] = 1.12 \times 10^{-4}$ and 4.20×10^{-5} mol cm^{-3}, respectively.

as a function of the imposed current, I, indicated that the fluxes of In(III) species were diffusion controlled. The In(III) diffusion coefficient was then computed from chronopotentiometric data according to Sand's law (Fig. 3):

$$\frac{I\tau^{1/2}}{C} = \frac{nFSD^{1/2}\pi^{1/2}}{2} \quad (5)$$

The results are summarised in Table 1. In addition, a logarithmic analysis of the chronopotentiograms is possible. The electrode potential varies linearly with $\log[(\tau/t)^{1/2} - 1]$, but the slope of the linear part of the curve (0.0746 V dec^{-1}) is slightly different from the theoretical value for a two electron reversible exchange process at 550 °C (0.0816 V dec^{-1}). Similar results were obtained when studying the oxidation of In(I) species (see Table 1).

All these criteria suggest that the kinetics of the In(III)/In(I) system are near to the limit for a reversible response.

3.2.1. Determination of the charge-transfer kinetic parameters. A detailed investigation of the kinetics of the In(III)/In(I) exchange was performed using both electrochemical reduction of In(III) and oxidation of In(I) ions at W and Mo, with similar results.

According to the previous results, the electro-reduction of In(III) involves one preceding diffusion step (diffusion of In(III) ions from the bulk solution to the electrode, characterized by the diffusion coefficient $D_{In(III)}$), one two electron transfer step (characterized by the charge transfer rate constant, k^o, and the charge–transfer coefficient, α), and a succeeding diffusion step (diffusion of In(I) ions electrogenerated from the electrode surface to the bulk). The kinetic parameters are, in practice, derived from the analysis of the semi-integral of the current [31].

The curves can then be analysed by using the equations corresponding to a reduction (Equation 6) and an oxidation (Equation 7) process both leading to soluble compounds:

$$E = E_1^o + \frac{2.3\,RT}{\alpha nF}\log\frac{k^o}{D^{1/2}} + \frac{2.3\,RT}{\alpha nF} \times \log\left[\frac{m^* - m - m\exp\left\{\frac{nF}{RT}\left(E - E_1^o\right)\right\}}{I}\right] \quad (6)$$

$$E = E_1^o + \frac{2.3\,RT}{\alpha nF}\log\frac{k^o}{D^{1/2}} + \frac{2.3\,RT}{\alpha nF} \times \log\left[\frac{\left(m^* - m\right)\exp\left\{\frac{nF}{RT}\left(E - E_1^o\right)\right\} - m}{I}\right] \quad (7)$$

where k^o and α are the change transfer rate constant and the transfer coefficient, respectively, and E_1^o the standard potential for the electrochemical In(III)/In(I) system, which was estimated from voltammetric measurements by applying the relationship $(E_{pa} + E_{pc})/2$ [32].

We have assumed the diffusion coefficients of In(III) and In(I) ions to be of similar value, as we have also demonstrated (Tables 1 and 4).

The average values of k^o and α obtained from the plot of E against the logarithmic function of the convoluted current are gathered in Table 2. According to the Matsuda and Ayabe criteria [33], in which the charge-transfer rate constant and the sweep rate

Table 1. Indium(III) and In(I) diffusion coefficients obtained on each substrate by different electrochemical techniques. Data resulting from the study of the electrochemical exchange In(III)/In(I)

Technique	$D_{In(III)}$ 10^6/cm^2 s^{-1}		$D_{In(I)}$ 10^6/cm^2 s^{-1}	
	Tungsten	*Molybdenum*	*Tungsten*	*Molybdenum*
Voltammetry	6.5 ± 0.2	7.6 ± 0.2	6.5 ± 0.2	6.1 ± 0.2
Semiintegral	7.1 ± 0.8	7.6 ±0.6	7.9 ± 1.2	7.2 ± 1.3
Chronopotentiometry	6.0 ± 0.2	7.3 ± 0.2	–	–

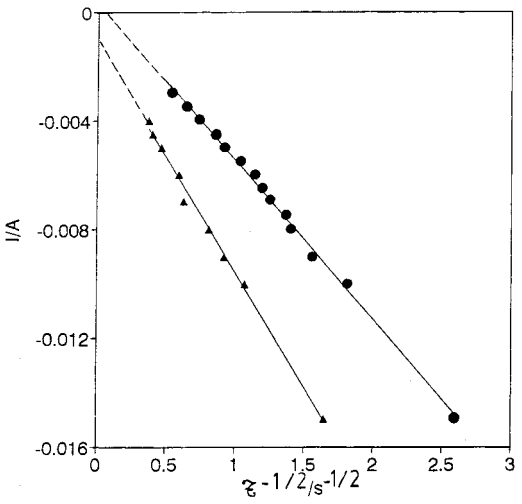

Fig. 3. Chronopotentiometric data of electroreduction of In(III) solutions. Verification of Sand's law. Key: (▲) tungsten and (●) molybdenum electrodes. [$InCl_3$] = 7.890×10^{-5} and 4.189×10^{-5} mol cm^{-3}, respectively.

are related, we can confirm that the exchange In(III)/In(I) can be qualified as quasi-reversible at both substrates studied.

To confirm these results, we used a simulation computer program (M271 COOL kinetic analysis software 1.10), for a quasireversible mechanism in which k^o, α, and the half-wave potential, $E_{1/2}$, were adjusted to give the best fit between the experimental and calculated results. We also tried to fit the system to a reversible process. However, the best results were found for a quasireversible process. Representative examples of these simulations are shown in Fig. 4 and the average values obtained are presented in Table 2. There is very good agreement between the different methods employed.

3.3. *Study of indium electrodeposition from InCl solutions*

The In(I)/In(0) exchange has been studied at metallic electrodes of W and Mo. As is shown in Fig. 5(a), the cathodic peak corresponding to the electroreduction of In(I) gives a steep rise and slow decay, and the anodic peak has the expected characteristics of a stripping peak, with the decay steeper than the rise. The ratios of the forward-to-reverse current peaks (I_{pc}/I_{pa}) are higher than unity, and the ratio (Q_c/Q_a) remains approximately constant at unity with increasing sweep rate, which indicates: (i) all the deposited material is removed electrochemically during the positive sweep, (ii) the indium adhesion to the electrode surface was good, and (iii) there are no conflicting chemical reactions coupled to the primary electrochemical process.

Overall, the voltammetric peaks for the deposition and stripping of indium at tungsten and molybdenum electrodes are unremarkable in appearance; however, in both cases the voltammetric curves recorded at different sweep rates, clearly show that the cathodic peak potential, E_{pc}, shifts negatively, (Fig. 5(b)), and the peak potential–half-peak potential separation, ($E_{pc} - E_{p/2}$), increases when the sweep rate is increased ($v > 0.2$ and 0.4 V s^{-1} at tungsten and molybdenum electrodes respectively) giving values higher than expected for a reversible and purely diffusion controlled process, suggesting some irreversibility of the In(I)/In(0) system.

To confirm these results we analysed the semiintegral of the current. The convoluted curves obtained at different sweep rates are very similar and exhibit well defined limiting currents, indicating that there is no gross change in the electrode surface area during the scan, that is, the indium deposit does not increase the

Table 2. Values of kinetic parameters for the In(III)/In(I) exchange obtained by different techniques at different substrates

Technique	*Tungsten*		*Molybdenum*	
	α	*log* k^o/cm s^{-1}	α	*log* k^o/cm s^{-1}
Kinetic Analysis software				
(In(III) reduction)	0.50 ± 0.02	−2.40 ± 0.10	0.58 ± 0.10	−2.40 ± 0.10
(In(I) oxidation)	0.44 ± 0.02	−2.46 ± 0.06	0.48 ± 0.05	−2.46 ± 0.06
Semiintegral				
(In(III) reduction)	0.56 ± 0.01	−2.53 ± 0.08	0.63 ± 0.02	−2.53 ± 0.08
(In(I) oxidation)	0.35 ± 0.04	−2.54 ± 0.06	0.32 ± 0.01	−2.54 ± 0.06

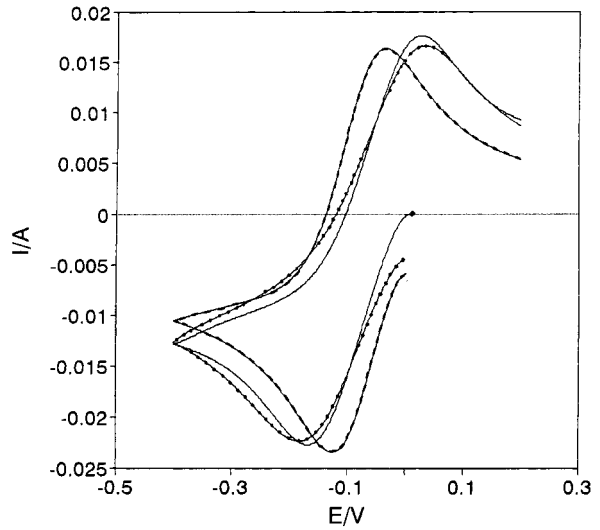

Fig. 4. Cyclic sweep voltammogram of $InCl_3$ reduction at a tungsten electrode. Sweep rate, 0.6 V s^{-1}. (—) experimental results; (••••) simulated results corresponding to a quasireversible process; (- - - - -) simulated results corresponding to a reversible process.

surface of the electrode to the point that it affects the limiting current for the In(I) reduction wave. Nevertheless, the convoluted voltammograms do not remain identical from the forward to the reverse scan, combined with the hysteresis behaviour between the forward and reverse sweeps, as can be observed in Fig. 6, showing a certain nonreversibility of the indium deposition.

When the convoluted curves were analysed further, the values of the kinetic parameters were obtained by plotting the logarithmic function of the convoluted curve as a function of E [34]:

$$E = E_2^{o} + \frac{RT}{\alpha nF}\ln k^{o} + \frac{RT}{\alpha nF}\ln A \qquad (8)$$

where A is given by

$$A = \left\{ \frac{(m^* - m)D^{-1/2} + nFS\exp\left(\frac{nF}{RT}(E - E_2^{o})\right)}{I} \right\} \qquad (9)$$

where E_2^{o} is the standard potential of the In(I)/In(0) system and was calculated from the voltammograms applying the following equation [35]:

$$E_p = E_2^{o} + 2.3\frac{RT}{nF}\log C - 0.849\frac{RT}{nF} \qquad (10)$$

at conditions where the electrochemical reaction is diffusion controlled.

According to the charge-transfer constant values so obtained and taking into account the Matsuda and Ayabe criteria [33], we can confirm that the In(I)/In(0) exchange is quasireversible at molybdenum and tungsten substrates (Table 3).

3.4. *Diffusion coefficient of In(I)*

The diffusion coefficient of of In(I) species was calculated from both electroreduction and oxidation of

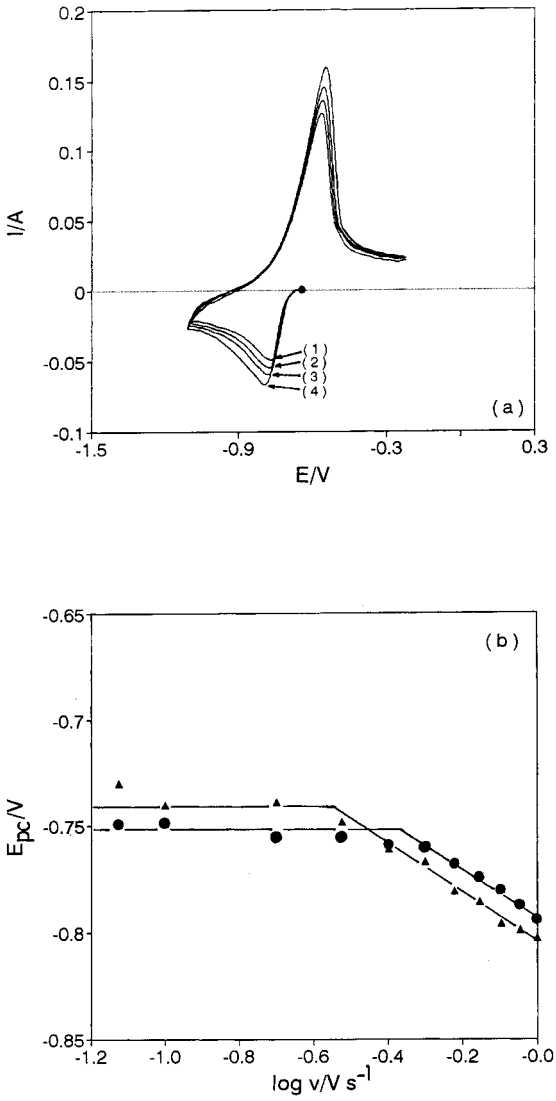

Fig. 5. (a) Cyclic voltammograms obtained on a molybdenum electrode showing the reduction of In(I). Sweep rates, v: (1) 0.6; (2) 0.7; (3) 0.8 and (4) 1.0 V s^{-1}. InCl concentration: 1.498×10^{-4} mol cm^{-3}. Electrode area 0.75 cm^2. (b) Variation of the cathodic peak potential with the logarithm of the sweep rate. Key: (▲) tungsten and (●) molybdenum electrodes. [InCl] = 2.859×10^{-4} and 1.498×10^{-4} mol cm^{-3}, respectively.

In(I) solutions. We have already referred to the calculations of $D_{In(I)}$, from oxidation of In(I) solutions (Section 3.2 and Table 1).

The values of $D_{In(I)}$, given in Table 4, were calculated by applying the Berzins–Delahay equation [35]:

$$I_p = 0.61\frac{(nF)^{3/2}}{(RT)^{1/2}}SCD^{1/2}v^{1/2} \qquad (11)$$

as well as using Equations 4 and 5.

Although tungsten or molybdenum wires were used as working electrodes, all the formulae used are defined according to planar semiinfinite diffusion because, under the experimental conditions, the corrections related to cylindrical geometry can be neglected [36–39]. On the other hand, most authors consider that the Berzins–Delahay equation for a reversible diffusion-controlled process can be used in the case of a quasireversible exchange, because, as

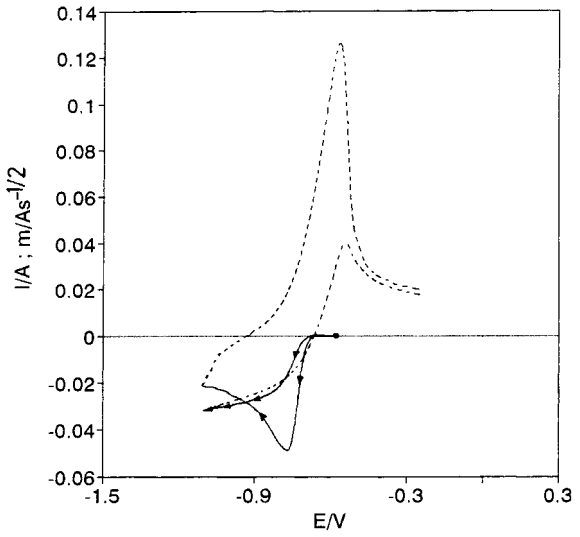

Fig. 6. Cyclic voltammograms and its corresponding convoluted curve for an In(I) solution on a molybdenum electrode. Sweep rate: 0.6 V s^{-1}. Reverse scans in dotted lines.

Table 3. Values of the kinetic parameters corresponding to the In(I)/In(0) exchange calculated by means of logarithmic analysis of the convoluted curves

	Tungsten	*Molybdenum*
α	0.6 ± 0.1	0.6 ± 0.1
log k^o/cm s^{-1}	−4.1 ± 0.4	−4.0 ± 0.1

Table 4. In(I) diffusion coefficients obtained by different electrochemical techniques at different solid substrates. Data obtained from the study of indium electrodepostion

Technique	$D_{In(I)}$ 10^6/cm^2 s^{-1}	
	Tungsten	*Molybdenum*
Voltammetry	6.4 ± 0.2	6.4 ± 0.2
Semiintegral	8.6 ± 0.2	8.7 ± 0.1
Chronopotentiometry	6.5 ± 0.2	7.0 ± 0.2
Chronoamperometry	6.1 ± 0.2	7.0 ± 0.2

long as the rate constant is high enough, I_p can be found from Equation 11.

It is also possible to calculate the diffusion coefficient from the I/t transients. The chronoamperograms obtained show a constant current due to thermal convection, for time values greater than 4 s. By plotting the variation of the current against $t^{-1/2}$ at potentials corresponding to the diffusion limiting current of the I/E reduction curve, it can be shown that the experimental data obey Cottrell's law:

$$I = nFSCD^{1/2}(\pi t)^{-1/2} \qquad (12)$$

The diffusion coefficient $D_{In(I)}$ (using a number of exchanged electrons $n = 1$) was calculated from the slope of the straight line obtained (Table 4).

The differences between these values are mainly related to the difficulty in determining the exact active electrode area. Therefore, it is possible to observe very good agreement between the different techniques employed.

3.5. *E–pO^{2-} diagram of In*

We carried out some experiments to measure the solubility product of indium oxides using an oxide-ion specific electrode based on an yttria-stabilized zirconia membrane.

In(III) was precipitated as oxide, and when the reaction was monitored using the zirconia electrode, an e.m.f. jump occurred at the point corresponding to the stoichiometric precipitation of the oxide [15].

The potential values obtained after successive additions of known amounts of sodium carbonate to a solution of In(III) with an initial concentration, $C = 0.0102$ mol kg^{-1}, are plotted in Fig. 7. Only one equivalence point can be observed, for a stoichiometric ratio $\alpha =$ [added carbonate]/[indium (III)] equal to 1.5. This indicates that the reaction is

$$2\ In^{3+} + 3\ O^{2-} \leftrightarrow In_2O_3(s)$$

The X-ray diffractometry analysis of the resulting solid compound recovered at the end of the experiment after dissolution of the melt in water and subsequent filtration, has shown the existence of In_2O_3, confirming the above reaction.

From the mass balance equations:

$$[O^{2-}]_{bulk} = [O^{2-}]_{add} - 3\ [In_2O_3]_{ppt} \qquad (13)$$

$$[In(III)]_{bulk} = [In(III)]_{initial} - 2\ [In_2O_3]_{ppt} \qquad (14)$$

and with the expression of the solubility product, $K_s = [In(III)]^2_{bulk}[O^{2-}]^3_{bulk}$, we can derive an equation for the titration curve.

$$[O^{2-}]^5 - 2C(\alpha - 3/2)[O^{2-}]^4 + C^2(\alpha - 3/2)^2[O^{2-}]^3 - 9/4\,K_s = 0 \qquad (15)$$

To obtain the value of $K_s(In_2O_3)$ from the experimental results, a simulation method based on these equations was used and led to arbitrary values of the constant. The simulated curve which best fits the experimental data is shown in Fig. 6. The mean value of $pK_s(In_2O_3)$ obtained was 14.2 ± 0.2 (molality scale).

When an attempt was made to experimentally determine the stability of In_2O by titration of a solution of In(I) with sodium carbonate with the zirconia electrode we could not see any e.m.f. jump corresponding to the In_2O formation, indicating that the In_2O is fully dissociated in this melt.

All the calculated data were used to construct the equilibrium potential–acidity diagram (Fig. 8), which summarises the chemical properties of indium compounds in the equimolar $CaCl_2$–NaCl mixture. By comparing this with the E–pO^{2-} diagram of the chlorinating mixtures $Cl_2(g) + O_2(g)$ and $HCl(g) + H_2O(g)$ previously determined [26], better conditions for the selective chlorination of indium oxides can be deduced. Thus, In_2O_3 can be chlorinated with the mixture $Cl_2 + O_2$ for $P(Cl_2) = 1$atm and

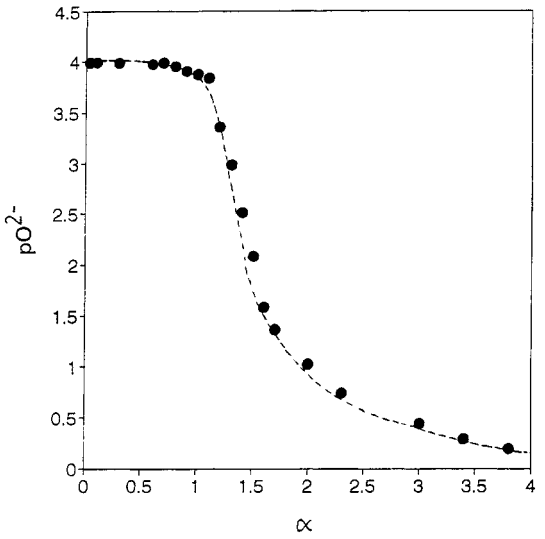

Fig. 7. Potentiometric titration of 0.1020 mol kg^{-1} In(III) solution by O^{-2} ions added as solid Na_2CO_3.

$P(O_2) = 10^{-3}$ and by bubbling HCl containing 1% water. In the first case, during the chlorination oxide ions are oxidised to gaseous oxygen, whereas in the second case, oxide ions are transformed into water by action of HCl, according to the following reactions:

$$3\,Cl_2(g) + In_2O_3(s) \leftrightarrow 2\,InCl_3(\text{dissolved}) + 3/2\,O_2(g)$$

$$6\,HCl(g) + In_2O_3(s) \leftrightarrow 2\,InCl_3(\text{dissolved}) + 3\,H_2O(g)$$

4. Conclusions

We have studied the chemical and electrochemical behaviour of indium ions, In(III) and In(I), in the equimolar $CaCl_2$–NaCl mixture at 550 °C using different substrates (i.e., tungsten and molybdenum) finding that metallic indium is liquid and stable in the melt.

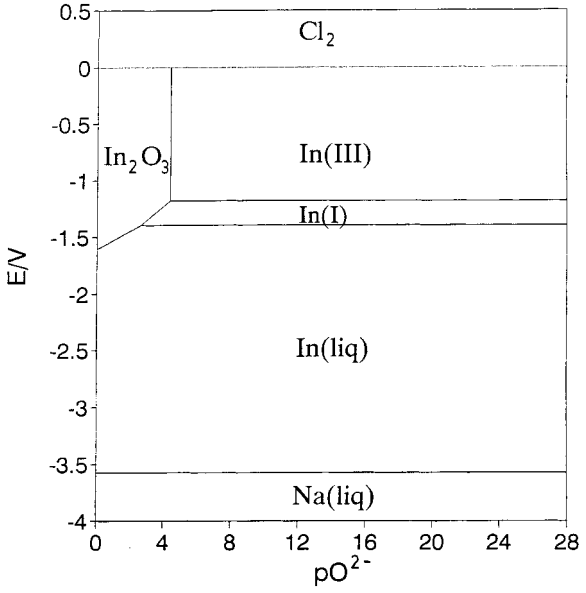

Fig. 8. Potential–pO^{2-} diagram for indium in equimolar $CaCl_2$–NaCl mixture at 550 °C. $[InCl_3] = [InCl] = 1$ mol kg^{-1}.

By using voltammetry it was demonstrated that the equilibrium:

$$InCl_3 + 2\,In \leftrightarrow 3\,InCl$$

is completely shifted to the right very quickly. This has been used to obtain stable In(I) solutions. Reduction of In(III) solutions lead to metallic indium in a two-step electrochemical exchange involving 2 and 1 electrons, respectively, which corresponds to the In(III)/In(I) and In(I)/In(0) systems.

Voltammograms corresponding to the electrochemical In(III)/In(I) exchange obtained from both oxidation of In(I) or reduction of In(III) solutions are well defined. The kinetic parameters, k^o and α, which characterise the electrochemical exchange, were obtained by applying the logarithmic analysis of the convoluted curves as well as a simulation program, showing that, according to the Matsuda and Ayabe criteria, the process can be considered quasireversible.

Electrodeposition of indium was uncomplicated at all the substrates studied. A very good adherence to the electrode materials of liquid indium, formed in the reduction process, was observed, with the formation of Na–In alloys for very reducing potentials. No evidence of indium dissolution into the melt was observed. Moreover, from the logarithmic analysis of the convoluted curves by applying the corresponding equation for an electrochemical exchange with the formation of an insoluble product, it was possible to calculate the charge rate constant values of the In(I)/In(0) electrochemical exchange showing that it is a quasireversible process. According to the Matsuda and Ayabe criteria the k^o values so obtained correspond closer to an irreversible behaviour than those from the In(III)/In(I) system. In addition, diffusion coefficients of In(III) and In(I) species are very similar and were calculated by different electrochemical techniques.

The solubility products of indium oxides were also investigated, indicating that In_2O is a strong oxide donor, being fully dissociated in the melt.

The chemical properties of indium compounds in the equimolar $CaCl_2$–NaCl mixture have been summarised in the form of an equilibrium potential–oxoacidity diagram, from which conditions for the selective chlorination of oxides can be deduced.

These results are step toward the objective of preparation of semiconducting thin films by electrodeposition, work that will continue in our laboratories.

Acknowledgements

The authors are grateful to DGES PB96-0364 (Spain) and to Junta de Castilla y León, C. de Educación y Cultura (Spain) for financial support. R.B. thanks CNRS (France) and E.U. (Leonardo da Vinci program) for two research grants. A.M.M. thanks DGICYT CE93-0017 (Spain) for a doctoral grant.

References

[1] H. Minoura, T. Negoro, M. Kitakata and Y. Ueno, *Sol. Energy Mater*. **12** (1985) 335.
[2] *Idem*, *ibid*. **147** (1987) 65.
[3] J. Shay and J. Wernick, 'Ternary Chalcopyrite Semiconductors: Growth, Electronic Properties and Application' (Pergamon, Oxford, 1975).
[4] R. A. Mickelsen and W. S. Chen, *Appl. Phys. Lett*. **36** (1980) 5.
[5] S. Menezes, *Appl. Phys. Lett*. **45** (1984) 148.
[6] H. A. Laitinen and C. H. Liu, *J. Am. Chem. Soc*. **80** (1958) 1015.
[7] B. N. Popov and J. V. Ivshin, *Croatia Chem. Acta* **60**(2) (1987) 315.
[8] J. M. Shafir and J. A Plambeck, *Can. J. Chem. Acta* **60**(2) (1987) 315.
[9] J. Bouteillon, M. Jafarian, J. C. Poignet and A. Reydet, *J. Electrochem. Soc*. **139**(1) (1992) 1.
[10] P. Pasquier, Thèse, Université P. et M. Curie Paris, France (1991).
[11] M. Mohamedi, Thèse, Institut National Polytechnique de Grenoble, France (1995).
[12] M. Taoumi, Thèse, Institut National Polytechnique de Grenoble, France, (1985).
[13] M. J. Barbier, J. Bouteillon and M. Taoumi, *J. Electrochem. Soc*. **133** (1986) 2502.
[14] U. Anders and J. A. Plambeck, *Can. J. Chem*. **47** (1969) 3055.
[15] Y. Castrillejo, M. A. García, E. Barrado, P. Pasquier and G. Picard, *Electrochim. Acta* **40** (1995) 2731.
[16] D. Ferry, Y. Castrillejo and G. Picard, *Electrochim. Acta* **33** (1988) 1661
[17] D. Ferry, Y. Castrillejo and G. Picard, *Electrochim. Acta* **34** (1989) 313
[18] D. Ferry, Y. Castrillejo and G. Picard, *J. Appl. Electrochem*. **23** (1993) 735
[19] Y. Castrillejo, D. Ferry, M. A. García, R. Pardo and P. S. Batanero, Material Science Forum **73–75**, edited by M. Chemla and D. Devilliers, (1991), p. 341.
[20] M. A. García, Y. Castrillejo, P. Pasquier and G. Picard, Molten Salt Forum, **1–2**, edited by C.A.C. Sequeira and G.S. Picard, (1993–94), p. 47.
[21] Y. Castrillejo, M. A. García, E. Barrado, P. Pasquier and G. Picard, *Electrochim. Acta* **40** (1995) 2731.
[22] Y. Castrillejo, A. M. Martínez, M. Vega, E. Barrado and G. Picard, *J. Electroanal. Chem* **397** (1995) 139.
[23] Y. Castrillejo, A. M. Martínez, G. M. Haarberg, B. Børresen, K. S. Osen and R. Tunold, *Electrochim. Acta* **42** (10) (1997) 1489.
[24] B. Trémillon, 'Electrochimie analytique et réaction en solution *in* Ed. Masson, *Reaction dans les sels Pondues*, Vol. 1, Ch. VII, Paris, France (1993) p. 324.
[25] P. L. Radloff and G. N. Papatheodorou, *J. Chem. Phys*. **72**(2) (1980) 992.
[26] A. M. Martínez, Y. Castrillejo, E. Barrado, G. M. Haarberg, and G. Picard, *J. Electroanal. Chem*., **449** (1998) 67–80.
[27] J. C. Gabriel, J. Bouteillon and J. C. Poignet, *J. Electrochem. Soc*. **141** (1994) 9.
[28] J. C. Imbeaux and J. B. Savéant, *Electroanal. Chem. Interfa. Electrochem*. **44** (1973) 169.
[29] G. Mamantov, D. L. Manning and J. M. Dale, *J. Electroanal. Chem*. **9** (1965) 253.
[30] A. J. Bard and L. R. Faulkner, 'Electrochemical Methods Fundamentals and Applications' (J. Wiley & Sons, New York, 1980).
[31] R. Greefs, R. Peat, L. M. Peter, D. Pletcher and J. Robinson, 'Instrumental Methods in Electrochemistry' (Ellis Horwood, London, 1990).
[32] M. Noel and K. I. Vasu, *in* 'Cyclic voltammetry and the frontiers of electrochemistry', Oxford & IBH (1990), p. 120.
[33] H. Matsuda and Y. Ayabe, *Z. Elektrochem*. (1954) 494.
[34] J. C. Myland and K. B. Oldham, *Anal. Chem*. **66** (1994) 1866.
[35] T. Berzins and P. Delahay, *J. Am. Chem. Soc*. **76** (1954) 555.
[36] Z. Galus, 'Fundamental of Electrochemical Analysis' (J. Wiley & Sons, New York, 1976).
[37] D. G. Peters and J. J. Lingane, *J. Electroanal. Chem*. **2** (1961) 1.
[38] K. B. Oldham, *ibid*. **41** (1973) 351.
[39] D. H.Evans and J. E. Price, *J. Electroanal. Chem*. **5** (1963) 77.